DOI 10.31489/2021No4/14-19

UDC 538.956

SYNTHESIS AND STRUCTURAL ANALYSIS OF NICKEL FERRITE SYNTHESIZED BY CO-PRECIPITATION METHOD

Durgadsimi S.U.[1], Kattimani V.R.[2], Maruti N.S.[3], Kulkarni A.B.[4,*], Mathad S.N.[5*]

[1]Department of Physics, Basaveshwar Engineering College, Bagalkot, Karnataka, India
[2]Department of Chemistry, Basaveshwar Engineering College, Bagalkot, Karnataka, India
[3]Department of Physics, K.R.C.E.S G.G.D Arts B.M.P Commerce and S.V.S Science college, Bailhongal, Karnataka, India
[4]Department of Physics, SKE Society's Govindram Seksaria Science College, Belagavi, Karnataka, India
[5]Department of Engineering Physics, K.L.E Institute of Technology, Hubballi, Karnataka, India,
physicssiddu@gmail.com

The Nickel ferrite has been synthesized by co-precipitation method. X-ray diffraction pattern confirms the formation of cubic spinel structure with lattice constant 8.347Å. Structural properties like X-ray density, average crystalline size, bond length, dislocation density and microstrain have been studied. The scanning electron microscope images show grain of bead structures. The Fourier transform infrared spectroscopy spectrum of nickel ferrite under investigation reveals the formation of a cubic spinel structure showing two significant absorption bands, corresponding to high frequency band $v_1$and low frequency band $v_2$arising from tetrahedral (A) and octahedral (B) interstitial sites respectively.

Keywords: Nickel ferrite, X-ray diffraction pattern, scanning electron microscope, Fourier transform infrared spectroscopy.

Introduction

Ferrites having a general chemical formula of AB_2O_4 with three types of ion distribution inside the structure namely, normal spinel, inverse spinel and mixed spinel [1]. The nickel ferrites are observed to be inverse spinel in nature, where nickel ion mainly occupying the tetrahedral site in the lattice. Structural, magnetic and electrical properties of ferrites are mainly dependent on synthesis conditions, size, metal ions in composition, and distribution of cations at tetrahedral A site and octahedral B sites [2]. The nickel ferrites are having large number of applications due to its good resistivity, good coercivity, good retentivity, optimum saturation magnetization, very high stability [3-4]. The nickel ferrites are found to good material in applications like memory storage devices, magnetic core [5], magnetic shielding [6], microwave devices [7-8], catalytic activity [9], gas sensor [10-12] etc. Nickel ferrites are synthesized using various methods based on the required properties, the methods are namely; auto- combustion method [13], sol-gel method [14], co-precipitation method [15-16], solid-state reaction method [17-18], hydrothermal [19] etc. In this paper, the work is aimed to synthesize $NiFe_2O_4$ nanoparticles by simple, low cost and environment friendly co-precipitation method. The co-precipitation method gives small grain size in the range of nm; the synthesis of particles takes place at room temperature [20]. The particle shape and size can be easily controllable based on the synthesis conditions. Hence Co-precipitation is comparatively having various advantages than other methods. The structural properties of synthesized material are characterized using X-ray diffraction, Scanning Electron Microscope (SEM) and Fourier transform infrared spectroscopy (FTIR).

1. Experimental part

The starting materials $NiCl_2$ and $FeCl_3$ were of analytical grade. The chemicals were taken in stoichiometric proportion; the mixture of chemicals is then dissolved in distilled water. The solution is thoroughly stirred for uniformity. The 3M NAOH is added drop wise for precipitation of solution with constant stirring at 60˚C. Oleic acid is added as surfactant to the solution. Obtained brown colour precipitate solution again stirred and then washed with distilled water and ethanol, and then filtered. The precipitate is centrifuged and dried; the dark brown colour product is finely powdered using agate mortar in acetone medium. The end product is annealed at 500˚Cfor 8 hours. The end product is annealed to give better crystallinity and agglomeration. The larger domain structures are helpful in better magnetic properties such

as coercivity and retentivity. The temperature of annealing is chosen keeping all these aspects and as per our previous work [21].The schematic diagram of synthesis is shown in Fig. 1. Structural characterization of the nickel ferrite powder was carried out on Philips X ray diffractometer (XRD), with Cu Kα radiation of wavelength 0.154nm. FTIR spectral analysis of sample was carried out in the wave numbers range between 400 cm^{-1} to 4000cm^{-1}.

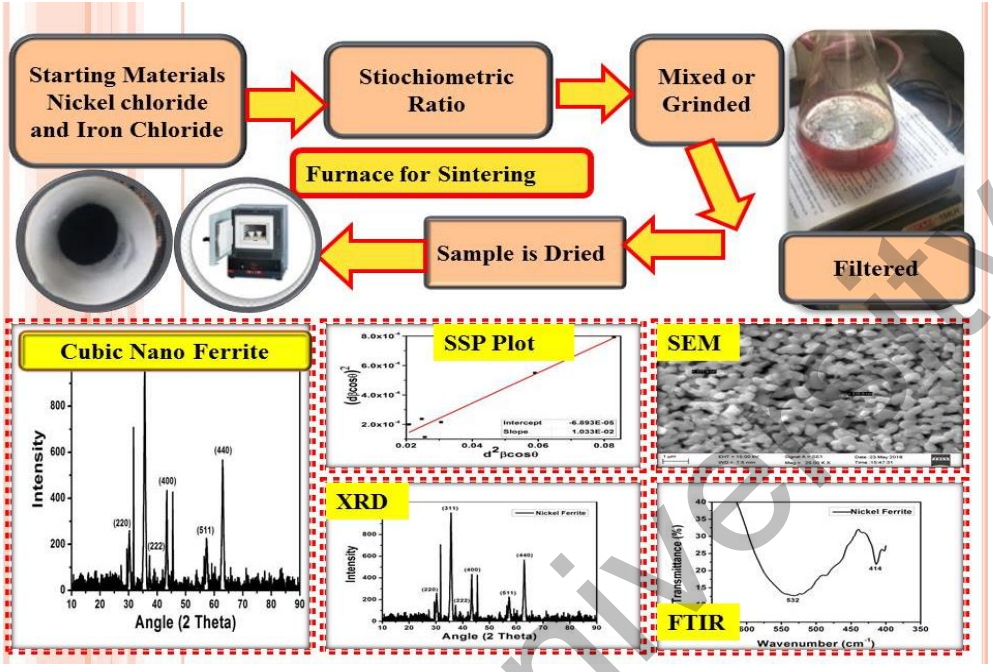

Fig.1. Schematic diagram of synthesis of characterization ferrite samples.

2. Results and discussion

2.1 X-Ray Diffraction Analysis

X-Ray Diffraction Analysis (XRD) pattern of synthesized $NiFe_2O_4$ is shown in Fig.2. Indexing of the peaks in XRD pattern is done by JCPDS card no.10-0325.Analysis of XRD pattern using Bragg's reflection planes (220),(311),(222),(400),(511)and (440) indicates the formation of cubic spinel structure. Interplanar spacing is calculated using Bragg's equation [17-18]

$$n\lambda = 2d\sin\theta, \quad (1)$$

where 'n' is order of diffraction, λ wavelength of x rays(0.154nm) and 'd' is interplanar spacing. For cubic spinel structure, interplanar spacing in terms of Miller indices is given by the equation

$$d=a/\sqrt{(h^2+k^2+l^2)}\ nm \quad (2)$$

Interplanar spacing 'd' and lattice constant 'a'are calculated with corresponding (hkl)values and are tabulated in table 1.

Table 1. Interplanar spacing and lattice constant.

(hkl)	Angle (2θ)	d(calculated) (Å)	d(observed) (Å)	Lattice constant(a) (Å)
(220)	30.31	2.950	2.949	8.341
(311)	35.65	2.518	2.518	8.352
(222)	37.36	2.410	2.407	8.338
(400)	43.41	2.087	2.085	8.338
(511)	57.27	1.605	1.609	8.358
(440)	62.92	1.475	1.477	8.355
				Lattice constant a = 8.347 (Å)

The calculated and observed values of 'd' are in good agreement for all the peaks. The deviation from the perfect crystallinity results into broadening of the diffraction peaks. In X-ray diffraction the formula which relates the crystallite size to the broadening of a peak in diffraction pattern is Debye-Scherrer's formula which is given by the equation

$$D = 0.9\lambda/(\beta \cos\theta), \quad (3)$$

where D is average crystallite size, λ wavelength of incident X-ray and β angular line width of half maximum intensity(FWHM).

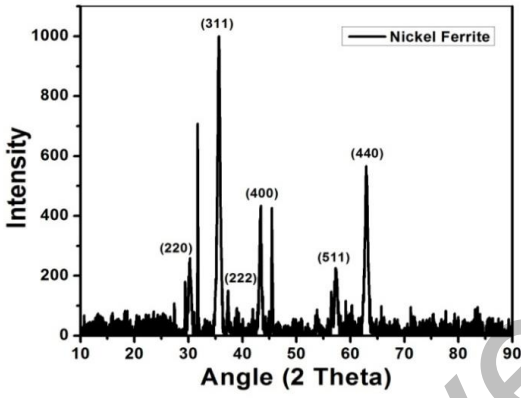

Fig.2.XRD pattern of $NiFe_2O_4$ nanoparticles

Dislocation density (δ) is defined as ratio of length of the dislocation lines the unit volume of the crystal, which represents the amount of defects in the sample and is calculated using equation (4)

$$\delta = 1/D^2 \quad (4)$$

The microstrain is defined as the deformation of an object divided by its effective length and is represented by 'ε'

$$\varepsilon = \beta\cos\theta/4 \quad (5)$$

X-ray density (d_x) and lattice constant 'a' are related by the following expression

$$d_x = 8M/N_A a^3, \quad (6)$$

where N_A is Avogadro number, M is the molecular weight of the nano nickel ferrite.

The distance between magnetic ions (hopping length) in tetrahedral A site (L_A) and octahedral B site (L_B) were calculated using the following relations

$$L_A = a\frac{\sqrt{3}}{4} \text{and} L_B = a\frac{\sqrt{2}}{4}, \quad (7)$$

where 'a' is lattice constant.

The calculated values of crystallite size (D), lattice constant (a), unit cell volume(V), dislocation density(δ), microstrain (ε), hopping lengths L_A and L_B and X-ray density (d_x) of $NiFe_2O_4$particles are tabulated in Table 2.

The size-strain broadening are additive components of the total breadth of a Bragg peak [22]. The distinct θ dependencies laid the basis for the separation of size and strain broadening in the analysis of Williamson and hall. The W-H plots are plotted using Eq.8 are plotted in Fig.3a.

$$\beta_{hkl}\cos\theta = \frac{K\cdot\lambda}{D} + 4\varepsilon\sin\theta \quad (8)$$

Table 2. Crystallite size, lattice constant, unit cell volume, dislocation density, microstrain (ε) hopping lengths (L_A and L_B) and X-ray density.

Crystallite Size (D) (Å)	182	
Lattice constant (a) (Å)	8.347	
Volume (a^3) ($Å^3$)	581	
Dislocation density (δ)(m^{-2})	$3.72x\ 10^{15}$	
Microstrain (ε) (m^2)	$2.06\ x\ 10^{-3}$	
Hopping Length (Å)	L_A = 3.614	L_B = 2.951
X-ray density(d_x) (g/cm^3)	5.353	

Williamson-Hall (WH) and Size Strain Plot (SSP).

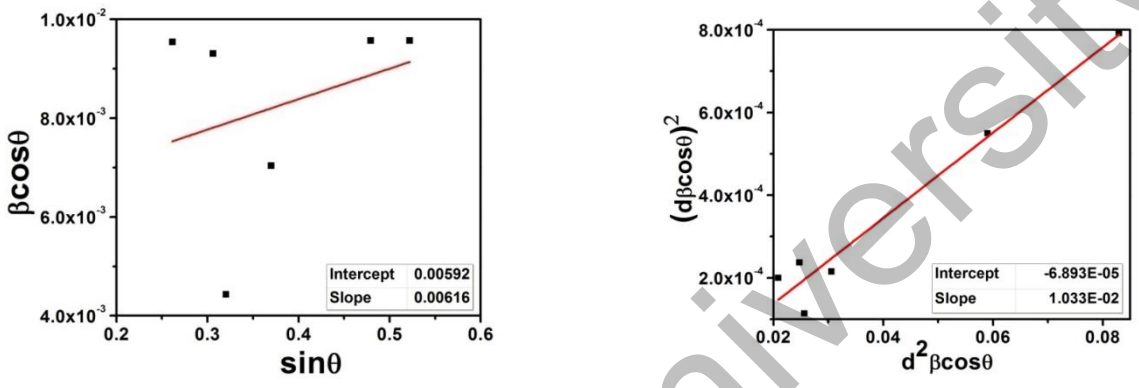

a) b)

Fig.3. (a) WH plots and (b) Size strain plots of $NiFe_2O_4$ ferrite

The evaluation of the SSP parameters are obtained by considering peaks in intermediate range. This gives less weight to data from high angle reflections where the precision is usually less. The SSP plots are shown in Fig.3b which is plotted using Eq.9. [23].

$$(d_{hkl}\beta_{hkl}\cos\theta)^2 = \frac{K.\lambda}{D}(d_{hkl}^2\beta_{hkl}\cos\theta) + \left(\frac{\varepsilon}{2}\right)^2 \quad (9)$$

Table.3 Crystallite size, micro strain and using W-H plots, SSP.

Crystallite size (in Å)		Micro strain (ε x 10^{-3})	
From W-H graph	From SSP graph	Micro strain ε=slope/4,(WH)	Micro strain ε=2*sqrt (intercept), (SSP)
234	134	1.54	16.60

2.2 Scanning Electron Microscope (SEM) analysis

The SEM image of $NiFe_2O_4$nano particles is shown in Fig.4. The particles are observed to be granular in shape and the size of particles lies in the range of 300-400 nm size. The particles show uniformity in size and showing partial agglomeration.

2.3 Fourier Transform Infrared (FTIR) Studies

Fig.5 shows the Fourier Transform Infrared (FTIR) spectrum of $NiFe_2O_4$.

Waldron [24] observed that both absorption bands of ferrites are due to the familiar tetrahedral octahedral M-O stretching vibration modes. The spectrum of $NiFe_2O_4$ ferrite under investigation reveals the formation of a cubic spinel structure showing two significant absorption bands, at 532 cm^{-1} and around 414 cm^{-1} corresponding to high frequency band $\nu_1$and low frequency band $\nu_2$arising from tetrahedral (A) and octahedral (B) interstitial sites respectively [25].

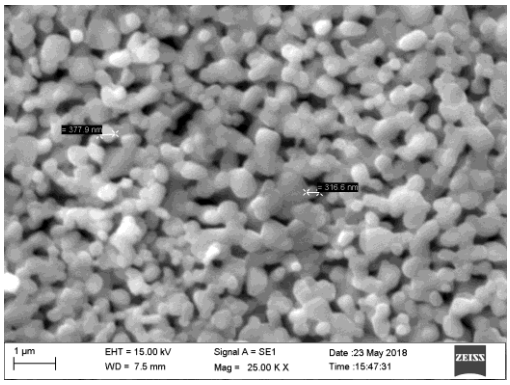

Fig.4. SEM image of $NiFe_2O_4$nano particles

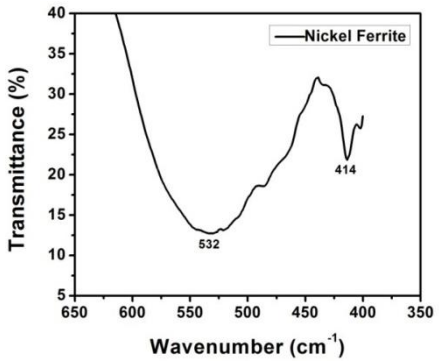

Fig.5. FTIR spectra of$NiFe_2O_4$

Conclusion

The spinel $NiFe_2O_4$ ferrite has been synthesized by Co- precipitation method. X-ray diffraction (XRD) pattern confirms the formation of cubic spinel structure with lattice constant 8.347Å.The crystalline size of the sample is observed to be 182Å (Debye-Scherrer method). The SEM images show grain of bead structures with size in the range 300-400 nm. The grains observed to be uniform in size but partially agglomerated. The two bands in FTIR spectra are observed at 532 cm^{-1} and 414 cm^{-1}confirming the tetrahedral and octahedral interstitial sites.

REFERENCES

1 Soohoo R.F. *Theory and Application of Ferrites*. 1960, 280 p.

2 Goldman A. *Modern ferrite technology*, 2006, 438 p.

3 Ranganathan, A. Ray Ferrites - what is new*? Pramana*. 2002, Vol. 58(5-6), pp. 995-1002.

4 Sugimoto M. The Past, Present, and Future of Ferrites. *J. Am. Cer. Soc*. 2004, Vol. 82(2), pp. 269-280.

5 Bahadur D., Giri J., Nayak B.B., et al. Processing, properties and some novel applications of magnetic nanoparticles. *Pramana*. 2005, Vol. 65(4), pp. 663-679.

6 Dar M.A., et.al, Surfactant assisted synthesis of Polythiophene/$Ni_{0.5}Zn_{0.5}Fe_{2-x}Ce_xO_4$ ferrite composites: Study of structural, dielectric and magnetic properties for EMI shielding applications. *Phy.Che.Che.Phy*. 2017, Vol.19, No.16, pp.1-35.

7 Bi K., Zhu W., Lei M., Zhou J. Magnetically tunable wideband microwave filter using ferrite-based metamaterials, *Appl. Phys. Lett.*, 2015, Vol. 106, No. 17, pp. 173507.

8 Su H., Zhang H., Tang X., Shi Y. Effects of microstructure on permeability and power loss characteristics of the NiZn ferrites, *J. Magn. Magn. Mater*. 2008, Vol. 320, No. 3-4, pp. 483-485.

9 Tsuji M., Kato H., Kodama T., Chang S. G., Hesegawa N., Tamaura Y., Methanation of CO_2 on H_2-reduced Ni(II)-or Co(II)-bearing ferrites at 200 C, *J. Mater. Sci.*, 1994, Vol. 29, No. 23, pp. 6227-6230.

10 Kamble R. B., Mathe V. L., Nanocrystalline nickel ferrite thick film as an efficient gas sensor at room temperature, *Sens. Actuators B: Chemical*, 2008, Vol. 131, No. 1, pp. 205-209.

11 Rezlescu E., et al. Porous nickel ferrite for semiconducting gas sensor *J. Phys.: Conf. Ser.* 2005, Vol. 15, pp. 51-54.

12 Darshane S. L., Suryavanshi S. S., Mulla I. S.,Nanostructured nickel ferrite: A liquid petroleum gas sensor, *Cer. Int.*, 2009, Vol. 35, pp. 1793-1797.

13 Tiwari R., De M., Tewari H. S., Ghoshal S. K., Structural and magnetic properties of tailored $NiFe_2O_4$ nanostructures synthesized using auto-combustion method, *Results in Physics*, 2020, Vol. 16, pp. 102916.

14 Raju G., Murali N., Prasad M.S.N.A., Suresh B., Kishore Babu B., Effect of chromium substitution on the structural and magnetic properties of cobalt ferrite, *Mater. Sci. Energy Tech.*, 2019, Vol. 2, No. 1, pp. 78-82.

15 Shivgurunathan P., Gibin S. R., Preparation and Characterization of Nickel nanoparticles via Co-precipitation method with citrate as chelating agent, *J. Mater. Sci.: Mater. Electronics*, 2016, Vol. 27, No. 3, pp. 2601-2607.

16 Shashidharagowda H., Mathad S. N., Effect of incorporation of copper on structural properties of spinel nickel manganites by co-precipitation method, *Mater. Sci. Energy Tech.*, 2020, Vol. 3, pp. 201–208.

17 KulkarniA. B., MathadS. N., Synthesis and Structural Analysis of Co–Zn–Cd Ferrite by Williamson–Hall and Size–Strain Plot Methods, *Int. J. Self-Prop. High-Temp. Synth.*, 2018, Vol. 27, No. 1, pp. 37–43.

18 Kulkarni A. B., Mathad S. N., Variation in structural and mechanical properties of Cd-doped Co-Zn ferrites, *Mater. Sci. Energy Tech.*, 2019, Vol. 2, pp. 455-462.

19 Jinendra U., et al. Template-free hydrothermal synthesis of hexa ferrite nano-particles and its adsorption capability for different organic dyes: Comparative adsorption studies, isotherms and kinetic studies, *Mater. Sci. Energy Tech.* 2019, Vol. 2, pp. 657-666.

20 Kulkarni A. B., et al. Influence of cadmium substitution on structural and mechanical properties of Co-Ni nano ferrite synthesized by co-precipitation method, *Macromol. Symp.*, 2020, Vol. 393, pp. 1900213 (1-7).

21 Kulkarni A. B., Mathad S. N., Effect of cadmium doping on structural and magnetic studies of Co-Ni ferrites, *Sci. sint.*,2021, Vol.53, pp. 1-11.

22 Zak K., Abrishami M. E., Majid W. H. A., Yousefi R., Hosseini S. M., X-ray analysis of ZnO nanoparticles by Williamson-Hall and size-strain plot methods, *Ceram. Inter.*, 2011, Vol. 37, pp 393-398.

23 Prabhu Y. T., et al. X-Ray Analysis by Williamson-Hall and Size-Strain Plot Methods of ZnO Nanoparticles with Fuel Variation, *World J. Nano Sci. Engg.*, 2014, Vol. 4, pp. 21-28.

24 Waldron R. D., Infrared spectra of ferrites, *Phys. Rev.*, 1955, Vol. 99, No. 6, pp. 1727-1765.

25 Rendale M. K., Mathad S. N. Puri V., Structural, mechanical and elastic properties of $Ni_{0.7-x}Co_xZn_{0.3}Fe_2O_4$ nano-ferrite thick films, *Microelectronics Int.*, 2017,Vol. 34,No. 2, pp. 57-63.

Article accepted for publication 10.08.2021